Noise Effect on Adaptive Command Shaping Methods for Flexible Manipulator Control

Sungsoo Rhim and Wayne J. Book

Abstract—**Since its introduction, the command shaping method has been applied to the control of many types of flexible manipulators and sthe effectiveness in the vibration suppression has been verified. However, designing an effective command shaper requires *a priori* knowledge about the system parameters. Recently, some efforts have been made to make the command shaper adapt to the changes in the system parameters. In this paper, the indirect and the direct adaptive command shaping methods in the time domain are compared, especially in terms of the noise effect on the performance. Analysis shows that the direct approach is less sensitive to the noise and this analytic result is verified by the proper simulation. Finally, experimental results using the direct approach are included.**

Index Terms—**Adaptive command shaping, flexible manipulator, noise, vibration.**

I. Introduction

FLEXIBILITY in a manipulator will degrade trajectory tracking control and manipulator tip positioning. In practice, however, constraints imposed by various operating requirements will render the presence of such flexibility unavoidable. The task that a manipulator must perform often leaves unspecified the exact path that the arm must follow. The general shape of the motion profile, the final position at the end of a path and the time necessary to bring the arm to rest at that position are far more important in these tasks. This fact makes it possible to place command shapers in the computer control which improve the flexible arm performance by suitably modifying the commands so that arm vibrations are minimized. Since [13] revived the concept of a dead-beat command design and extended it to a more sophisticated command shaping approach, the command shaping method using time-delay filters has been applied in many applications and its effectiveness in suppressing the residual vibration has been verified. The design of an effective command shaper, however, requires *a priori* knowledge of flexible system parameters such as the natural frequency and the damping ratio of the undesired elastic mode.

When the command shaping method is used to control flexible manipulators with uncertainty of system parameters, there are two approaches that can be taken [1]. The first approach is to design command shapers as robust as possible based on the available information on a given system (e.g., expected variation range of the natural frequency) [11]. Unfortunately, the robustness of the shaper comes at the expense of the command shaper length, which means more delay in the response. Moreover, this approach still requires a fair amount of *a priori* knowledge about the system parameters for proper design. The second approach is to make the command shaper adapt to uncertain or varying system parameters. The indirect adaptive command shaping method has focused on the system identification either in the frequency domain [3], [14] or in the time domain [2], [8]. In these approaches, new filter coefficients are calculated using the system estimation results. Thus the effectiveness of the updated command shaper relies on the quality of the system estimation results. Direct adaptation algorithms can also be used, where system parameters are never explicitly utilized. Among time-delay filter parameters that can be adapted in the direct adaptation are 1) the number of terms in the filter; 2) the time delay of the filter; 3) the coefficients of the terms. The number of terms has not been adapted on-line in previous works. The authors will fix the number of terms at three for a single mode throughout the following discussion. It is known that the adaptation of time delay of an finite impulse response (FIR) filter is a very complicated nonlinear problem. However, this difficult nonlinear approach can be avoided by utilizing the characteristics of a three-impulse command shaper called optimal arbitrary time-delay filter (OATF). The OATF provides the freedom in choosing the time delay regardless of the system parameters [6]. Recently, based on this unique characteristic of the OATF, the authors proposed a direct adaptive command shaping method which can adapt only the filter coefficients leaving fixed the number of impulses and the time delay to minimize the residual vibration [9].

In this paper, we compare two time-domain adaptive command shaping approaches (the indirect and the direct), particularly in terms of the noise effect on the performance. The noise effect on both approaches is analyzed and the analytic result is supported by a set of appropriate simulations. Also, an experiment using the direct approach is performed and its results are included at the end.

Manuscript received July 21, 2000; revised September 1, 2000. Recommended by Guest Editors S. O. R. Moheimani and G. C. Goodwin. This work was supported in part by Visteon Automotive Systems and CAMotion, Inc.

S. Rhim is with CAMotion, Inc., Atlanta, GA 30318, USA (e-mail: sungsoo.rhim@camotion.com).

W. J. Book is with School of Mechanical Engineering, Georgia Institute of Technology, Atlanta, GA 30332 USA (e-mail: wayne.book@me.gatech.edu).

Publisher Item Identifier S 1063-6536(01)00419-5.

II. Dynamics of Flexible Manipulator

The system of interest to this work is the gantry-type robot with a prismatic joint and single flexible link shown schematically in Fig. 1. $u(t)$ denotes the control force as a function of time, t. The length of the flexible link is L. The x-w coordinate frame is attached to the prismatic joint and moves with the

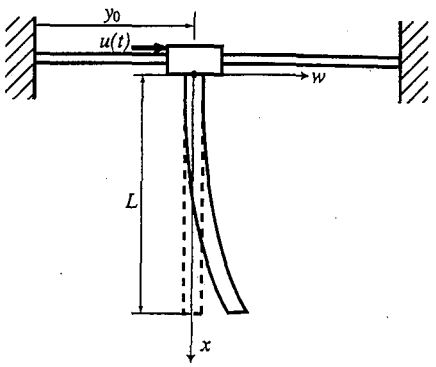

Fig. 1. Schematic diagram of a gantry robot with a flexible link.

flexible link. $y_0(t)$ represents the horizontal displacement of the joint. Then, the horizontal displacement of the flexible link at a given value of x can be expressed as

$$y(t,x) = y_0(t) + w(t,x). \tag{1}$$

The flexible link system consists of an infinite number of modes. For practical purposes, however, we assume that we are able to characterize the system's behavior well enough with only N modes. Using the method of assumed modes, we thus have

$$y(t,x) = \sum_{i=1}^{N} q_i(t)\phi_i(x) \tag{2}$$

where $q_i(t)$ are generalized coordinates and $\phi_i(x)$ are basis functions or assumed mode shapes. Then, e.g., by using Lagrange's equations, we find that the system's equations of motion are given by

$$\mathbf{M}\ddot{\mathbf{q}}(t) + \mathbf{D}\dot{\mathbf{q}}(t) + \mathbf{K}\mathbf{q}(t) = \mathbf{B}u(t) \tag{3}$$

where

$$\mathbf{M} \equiv \begin{bmatrix} M_r & \mathbf{M}_{re} \\ \mathbf{M}_{re}^T & \mathbf{M}_e \end{bmatrix}, \quad \mathbf{K} \equiv \begin{bmatrix} 0 & \mathbf{0} \\ \mathbf{0} & \mathbf{K}_e \end{bmatrix}$$
$$\mathbf{D} = \alpha\mathbf{M} + \beta\mathbf{K}, \quad \mathbf{B} = \begin{bmatrix} B_r \\ \mathbf{B}_e \end{bmatrix}$$

α and β are constants, and $\mathbf{q}(t) = [q_r(t)\ \ \mathbf{q}_e(t)]^T$, where $q_r(t)$ is the rigid generalized coordinate (representing the joint motion or rigid mode) and $\mathbf{q}_e(t)$ are the flexible generalized coordinates (representing the elastic motion or mode). The subscripts r and e in the above equations denote rigid body motion and elastic motion, respectively; $\mathbf{M}_{re}$ represents coupling between the rigid mode and the elastic modes. Only one rigid mode appears in the above equation corresponding to the horizontal translation. Generally, the mass matrix $\mathbf{M}$ and the stiffness matrix $\mathbf{K}$ may vary with the system configuration $\mathbf{q}(t)$. However, for our gantry-type manipulator, these matrices are constant. The manipulator joint displacement, $y_{\text{joint}}(t)$, and the tip displacement, $y_{\text{tip}}(t)$, are expressed in terms of the generalized coordinates by

$$\mathbf{y}(t) \equiv \begin{bmatrix} y_{\text{joint}}(t) \\ y_{\text{tip}}(t) \end{bmatrix} = \begin{bmatrix} \mathbf{\Phi}^T(0) \\ \mathbf{\Phi}^T(L) \end{bmatrix} \mathbf{q}(t) \tag{4}$$

where $\mathbf{\Phi}(x)^T = [\phi_1(x)\ \phi_2(x)\ \cdots\ \phi_N(x)]$. Next, we proceed to derive the transfer functions between the control force, $u(t)$, and the outputs $\mathbf{y}(t)$. Assuming the use of a set of mode shapes such that $\phi_i(0) = 0$ for $i \neq 1$, we get $B_r = 1$ and $\mathbf{B}_e = \mathbf{0}$. With these mode shapes, the rigid motion (or the joint motion) is represented solely by the first mode and the first generalized coordinate. Without losing generality, these particular values of $\mathbf{B}$ matrix elements are used for the simplicity in the following derivation.

First, we observe that

$$\frac{Q_r(s)}{U(s)} = \frac{1 - (s^2\mathbf{M}_e + s\mathbf{D}_{22} + \mathbf{K}_{22})^{-1}(s\mathbf{D}_{12}\mathbf{K}_{12})\mathbf{B}_2}{s^2 M_r + sD_{11}} \tag{5}$$

and

$$\frac{\mathbf{Q}_e(s)}{U(s)} = (s^2\mathbf{M}_e + s\mathbf{D}_{22} + \mathbf{K}_{22})^{-1}\mathbf{B}_2 \tag{6}$$

where s is the Laplace variable and, e.g., $Q_r(s)$ is the Laplace transform of $q_r(t)$. Also

$$D_{11} = \alpha M_r, \quad \mathbf{D}_{12} = -\beta\mathbf{M}_{re}\mathbf{M}_e^{-1}\mathbf{K}_e$$
$$\mathbf{D}_{22} = \alpha\mathbf{M}_e + \beta\mathbf{K}_e, \quad \mathbf{K}_{12} = -\mathbf{M}_{re}\mathbf{M}_e^{-1}\mathbf{K}_e$$
$$\mathbf{K}_{22} = \mathbf{K}_e, \quad \text{and} \quad \mathbf{B}_2 = -\mathbf{M}_{re}^T/M_r.$$

Then, using (4), we obtain the transfer functions $G_{\text{joint}}(s) \equiv Y_{\text{joint}}(s)/U(s)$ and $G_{\text{tip}}(s) \equiv Y_{\text{tip}}(s)/U(s)$:

$$\begin{bmatrix} G_{\text{joint}}(s) \\ G_{\text{tip}}(s) \end{bmatrix} = \begin{bmatrix} \Phi^T(0) \\ \Phi^T(L) \end{bmatrix} \begin{bmatrix} Q_r(s)/U(s) \\ \mathbf{Q}_e(s)/U(s) \end{bmatrix}. \tag{7}$$

III. Command Shaping

The *command shaper* reshapes the desired input to a flexible system such that the resonances of the elastic system modes are not excited. It takes the form of an FIR filter, with filter parameters determined by the resonant frequencies and the damping ratios of the undesired elastic modes of the flexible system. In this research we have used a particular *three-term* command shaper called the OATF)[6]. For a single elastic mode cancellation, an OATF is given by the following equation:

$$c(t) \equiv \frac{1}{M}\{\delta(t) - 2\cos(\omega_d T_d)e^{-\zeta\omega_n T_d}\delta(t - T_d) + e^{-2\zeta\omega_n T_d}\delta(t - 2T_d)\} \tag{8}$$

where

- T_d time delay;
- $\delta(t)$ unit impulse function centered at $t = 0$;
- ω_n natural frequency of the undesired elastic mode;
- ζ corresponding damping ratio;
- ω_d corresponding damped natural frequency, and $M \equiv 1 - 2\cos(\omega_d T_d)e^{-\zeta\omega_n T_d} + e^{-2\zeta\omega_n T_d}$.

In order to have the same total steady-state response both before and after the command shaping of the input, the command shaper is normalized to have unit dc gain. It has been shown that if the command shaper coefficients are properly chosen, the OATF is capable of canceling the given resonance poles with its zeros using any T_d; note that this is not true for earlier command shaping methods [6].

When we realize command shaping in the discrete-time domain, the time delay T_d is not permitted to be an arbitrary number. Instead, it must be chosen as an integer multiple of the plant sampling time, T_s. The freedom of the OATF in choosing the time-delay makes it easy to implement in a digital control system. The z-domain representation of the OATF is given by

$$C(z) \equiv \frac{1}{M}(1 - 2\cos(\omega_d T_d)e^{-\zeta\omega_n T_d}z^{-\Delta} + e^{-2\zeta\omega_n T_d}z^{-2\Delta}) \tag{9}$$

where Δ = integer $= T_d/T_s$.

IV. Noise Effect on Adaptive Command Shaping

If system parameters change, the corresponding change in desired command shaper parameters can be readily calculated. The indirect adaptation process can then be conceived that identifies system parameters (natural frequency and damping ratio), calculates improved command shaper parameters and changes them.

The selection of the identification method between the parameterized (time domain) method and the nonparameterized (frequency domain) method should depend on, first of all, what kind of prior knowledge (expected frequency range, system order, system structure) is available. Since the eventual goal of the system identification in the adaptive command shaping is to get an effective command shaper whose structure can be fixed, we can utilize this information of the filter structure to adapt only the filter coefficients directly in the time domain. For the frequency-domain approach, even though there are several efficient algorithms developed, it is still a computational burden to do an FFT analysis during the control calculation. Even after the spectrum is obtained, further processing is required to identify the peaks in its magnitude and estimate the damping ratio.

Considering these advantages, the authors focus on the comparison of two time-domain adaptive command shaping approaches (indirect and direct) that use the least squares algorithm. Particularly, the comparison is made in terms of the noise effect on the performance of adaptive command shapers.

A. Noise Effect on Time Domain System Identification Method

A linear time-invariant system with additive disturbance can be specified in the discrete-time domain by two transfer functions $G(z)$, $H(z)$ and a noise $e(n)$ as (10)

$$y(n) = G(z)u(n) + H(z)e(n) \tag{10}$$

where

- $u(n)$ input to the system;
- $y(n)$ output of the system;
- $G(z)$ system model defined as $G(z) = \sum_{k=1}^{\infty} g(k)z^{-k}$;
- $H(z)$ noise model defined as $H(z) = 1 + \sum_{k=1}^{\infty} h(k)z^{-k}$, and n = given discrete time.

(Throughout this paper, for practicality we switch freely between the discrete filter form and its z-transform by using z both for the delay operator on the discrete-time signal and for the z-transform variable.) We assume that the noise $e(n)$ is random signal with zero mean value and the noise model $H(z)$ and its inverse are both stable.

The system identification (or estimation) is to determine a set of system parameters (such as coefficients $g(k)$ and $h(k)$ of $G(z)$ and $H(z)$) in the given system representation based on a certain criterion. For the following discussion, let us represent this set of system parameters with θ. At a given discrete-time n, the one-step-ahead prediction of the system (10) can be calculated as below [5]

$$\hat{y}(n) = \hat{H}^{-1}(z,\theta)\hat{G}(z,\theta)u(n) + [1 - \hat{H}^{-1}(z,\theta)]y(n) \tag{11}$$

where $\hat{H}(z,\theta)$ and $\hat{G}(z,\theta)$ represent the estimation of $H(z)$ and $G(z)$ based on a certain choice of the system parameter set θ respectively. The optimal estimation of θ can be obtained by minimizing a given cost function, which evaluates the difference between the estimated system and the observed data. In this paper, as the cost function we consider the quadratic norm of the prediction error shown below

$$J(N) = \frac{1}{N}\sum_{n=1}^{N}\varepsilon^2(n) \tag{12}$$

where the prediction error $\varepsilon(n)$ is defined as $\varepsilon(n) = y(n) - \hat{y}(n)$. By substituting (11), the prediction error can be rewritten as

$$\varepsilon(n) = \hat{H}^{-1}(z,\theta)[y(n) - \hat{G}(z,\theta)u(n)]. \tag{13}$$

Following [5], with a large N this quadratic cost function can be transformed to the frequency domain and can be expressed approximately as

$$J(N) \approx \frac{1}{N}\sum_{k=0}^{N-1}\left|G_N\left(W_N^k\right) - \hat{G}(e^{j\omega},\theta)\right|^2 \times \left|U_N\left(W_N^k\right)\right|^2 |\hat{H}^{-1}(e^{j\omega},\theta)|^2 \tag{14}$$

where $W_N^k \equiv e^{j2\pi k/N}$ and $G_N(W_N^k)$ is an empirical transfer function estimate of the system, which is defined as

$$G_N\left(W_N^k\right) = Y_N\left(W_N^k\right)/U_N\left(W_N^k\right). \tag{15}$$

For distinction, we have used argument W_N^k for the DFT and $e^{j\omega}$ for the transfer function evaluated at the point $z = e^{j\omega}$, for $-\pi \le \omega \le \pi$. Consequently, the optimal θ is obtained by fitting the estimated transfer function $\hat{G}(e^{j\omega},\theta)$ to the empirical transfer function $G_N(W_N^k)$ with a weighted norm. Notice that the inverse of the noise model spectrum, $|\hat{H}^{-1}(e^{j\omega},\theta)|^2$, and the input spectrum, $|U_N(W_N^k)|^2$, are weighting the cost function.

B. Indirect Adaptive Command Shaping

In the indirect adaptive command shaping approach, the flexible manipulator system is estimated first, then new coefficients of the command shaper are calculated based on system parameters (ω_n, ζ) extracted from the system estimation result. Therefore, the effectiveness of the updated command shaper entirely relies on the quality of the system estimation result. The block diagram of this approach is given in Fig. 2.

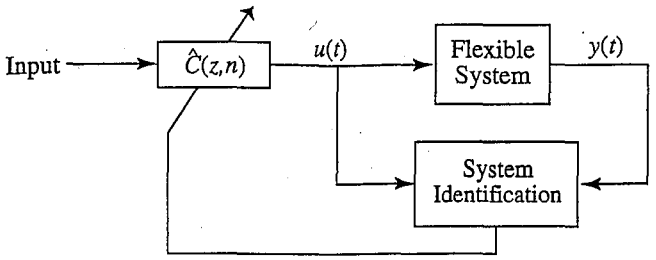

Fig. 2. Block diagram of indirect adaptive command shaping.

For the system estimation, first of all, we need to choose a model for the system. While the analysis in the previous section can be applied to other types of time-domain estimation models, here we consider linear regressor models where the prediction can be expressed in a linear regression form. This kind of model (ARX, ARARX, ...) is the most favored in many applications, because the linearity of the prediction allows the use of powerful and simple linear techniques. From among those, the ARX model is used for the discussion following. Using the ARX model, the flexible manipulator system including the noise can be expressed as

$$A(z)y(n) = B(z)u(n) + e(n) \tag{16}$$

where $A(z) \equiv 1 + a_1 z^{-1} + \cdots + a_{n_a} z^{-n_a}$, $B(z) \equiv b_1 z^{-1} + \cdots + b_{n_b} z^{-n_b}$, and $e(n)$ = zero mean random noise. Let us define the system parameter vector θ and the regressor vector ψThen, by comparing (16) with (10) in the previous section, the estimated system description is

$$\hat{G}(z,\theta) = \frac{\hat{B}(z,\theta)}{\hat{A}(z,\theta)}, \quad \hat{H}(z,\theta) = \frac{1}{\hat{A}(z,\theta)}. \tag{17}$$

and the predictor can be expressed as

$$\hat{y}(n) = \hat{B}(z,\theta)u(n) + [1 - \hat{A}(z,\theta)]y(n) \tag{18}$$

or in a linear regressor form

$$\hat{y}(n) = \theta^T(n)\psi(n) = \psi^T(n)\theta(n) \tag{19}$$

where

$$\begin{aligned}\theta^T(n) &= [-a_1(n) \quad \cdots \quad -a_{n_a}(n) \\ &\qquad b_1(n) \quad \cdots \quad b_{n_b}(n)] \\ \psi^T(n) &= [y(n-1) \quad \cdots \quad y(n-n_a) \\ &\qquad u(n-1) \quad \cdots \quad u(n-n_b)].\end{aligned}$$

Substituting (17) into (14), we can get the frequency domain representation of the quadratic cost function for ARX model as

$$\begin{aligned}J(N) \approx \frac{1}{N}\sum_{k=0}^{N-1} &\left|G_N\left(W_N^k\right) - \hat{G}(e^{j\omega},\theta)\right|^2 \\ &\times \left|U\left(W_N^k\right)\right|^2 |\hat{A}(e^{j\omega},\theta)|^2.\end{aligned} \tag{20}$$

Notice that the square of the difference between the estimated transfer function and the empirically obtained system transfer function, $|G_N(W_N^k) - \hat{G}(e^{j\omega},\theta)|^2$, is weighted by $|U(W_N^k)|^2$ and $|\hat{A}(e^{j\omega},\theta)|^2$. Inclusion of $|\hat{A}(e^{j\omega},\theta)|^2$ is the result of

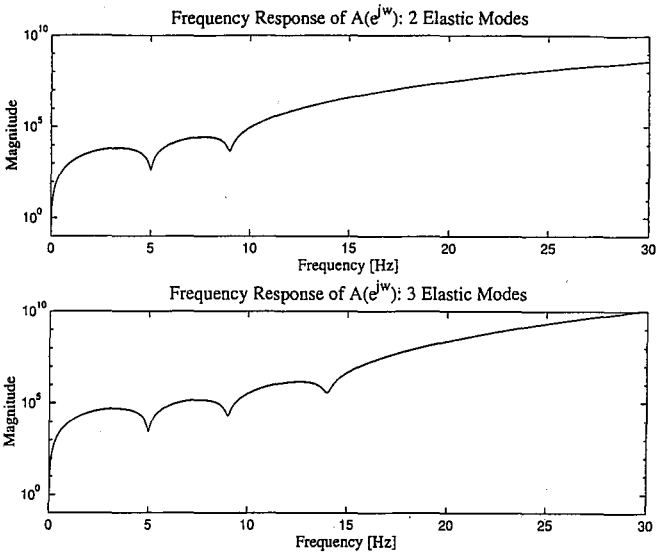

Fig. 3. Frequency response magnitude of denominator polynomial $A(z)$.

choosing an ARX model for the estimation. However, for any other type of linear regressor model with the obtainable regressor $\psi(n)$, this term will be included in the cost function, too.

The magnitude of $A(e^{j\omega})$ increases with frequency. The higher the order of $A(z)$, the more rapidly the magnitude of $A(e^{j\omega})$ increases with frequency. As an example, Fig. 3 shows frequency responses of $A(z)$ for two lightly damped links with two elastic modes (natural frequencies at 5 Hz and 9 Hz) and three elastic modes (natural frequencies at 5 Hz, 9 Hz, and 14 Hz), respectively. Thus, this estimation algorithm gives a very heavy weighting to the highest frequencies where the the empirical estimation is dominated by noise. Generally speaking, minimization of the cost function will clearly result in a estimated transfer function $\hat{G}(e^{j\omega},\theta)$ with too large a high-frequency gain at the expense of accuracy in the region of critical interest (poles of $G_N(W_N^k)$).

A solution to this weighting problem is to use the filtered prediction error $\varepsilon_F(n)$ shown below instead of $\varepsilon(n)$ for the performance index [10].

$$\begin{aligned}\varepsilon_F(n) &\equiv L(z)\varepsilon(n) = L(z)\{y(n) - \hat{y}(n)\} \\ &= L(z)\{y(n) - \hat{B}(z,\theta)u(n) - [1 - \hat{A}(z,\theta)]y(n)\} \\ &= -\hat{B}(z,\theta)L(z)u(n) + \hat{A}(z,\theta)L(z)y(n).\end{aligned}$$

The effect of prefiltering $\varepsilon(n)$ with a filter $L(z)$ is identical to changing the noise model from $\hat{H}(z,\theta)$ to $L^{-1}(z)\hat{H}(z,\theta)$. Consequently, the cost function is altered to be

$$\begin{aligned}J(N) \approx \frac{1}{N}\sum_{k=0}^{N-1} &\left|G_N\left(W_N^k\right) - \hat{G}(e^{j\omega},\theta)\right|^2 \\ &\times \left|U\left(W_N^k\right)\right|^2 |L(e^{j\omega})\hat{A}(e^{j\omega},\theta)|^2.\end{aligned} \tag{21}$$

However, this solution introduces other problems such as how to design a proper filter $L(z)$ to cancel the effect of $|\hat{A}(e^{j\omega},\theta)|^2$ without knowing the system parameters and extra signal processing time. Besides that, the cost function still has the weighting by the input spectrum $|U(W_N^k)|^2$. In some cases,

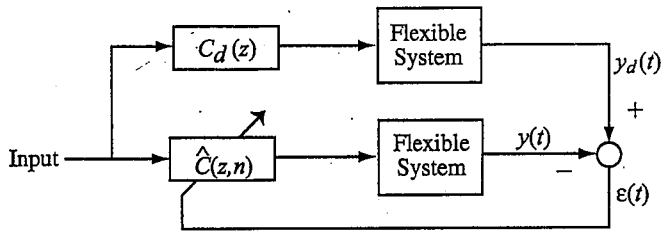

Fig. 4. Prefiltering configuration.

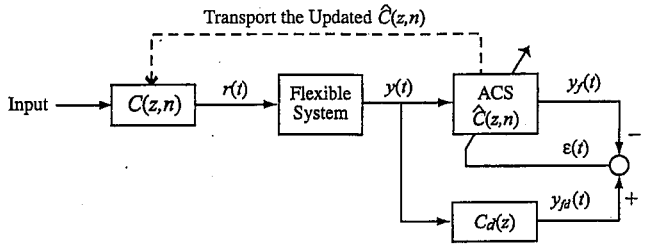

Fig. 5. Postfiltering configuration.

this could result in a bad estimation in the frequency range of interest.

C. Direct Adaptive Command Shaping

In the direct adaptive command shaping approach, we directly estimate the coefficients of the desired command shaper $C_d(z)$ without seeking any information about the system parameters. As mentioned before, even without knowing the system parameters, we can fix the time-delay T_d or Δ of command shaper to cancel a given elastic mode. Although the number of impulses and the time delay could vary during the direct adaptive approach, in this paper we have fixed the number of impulses (three for a single elastic mode) and the time delay during the adaptation. With fixed time delay and the unity gain constraint, only two coefficients are left to be adapted for a single mode vibration cancellation. The adaptive command shaper $\hat{C}(z,n)$ has the structure of the OATF shown in (9) with variable coefficients to be adapted.

$$\hat{C}(z,n) = \hat{c}_0(n) + \hat{c}_1(n)z^{-\Delta} + \hat{c}_2(n)z^{-2\Delta} \qquad (22)$$

where $\sum_{i=0}^{2} \hat{c}_i = 1$ (unity gain constraint).

Now, let us think about the proper configuration for the adaptive filtering algorithm.

The configuration shown in Fig. 4 is perhaps the most straightforward configuration. However, with this configuration we cannot use recursive least squares (RLS) or other high-speed adaptive processes based on the linear regressor model which allows the use of powerful linear techniques. To be able to use such linear techniques in the adaptive filtering, we need to have an prediction error defined by the difference between the output of desired filter and the output of the actual filter instead of the outputs of the plant. Alternatively, the plant and the feedforward shaper are commuted (interchanged in order in the block diagram) with the assumption of linearity so that the error $\varepsilon(n)$ is directly available from the adaptive shaper output as shown in Fig. 5. If the command shaper and the flexible system are linear, the shaper generated by the postfiltering configuration will also be optimal for the prefiltering configuration. In the post filtering configuration of Fig. 5, the adapted command shaper $\hat{C}(z,n)$ is copied to $C(z,n)$ which actually reshapes the command that goes into the flexible manipulator system $G_{cl}(z)$. In the postfiltering configuration, the ARX model of the desired command shaper output, $y_{df}(n)$ is represented as

$$y_{fd}(n) = C_d(z)y(n) + e(n). \qquad (23)$$

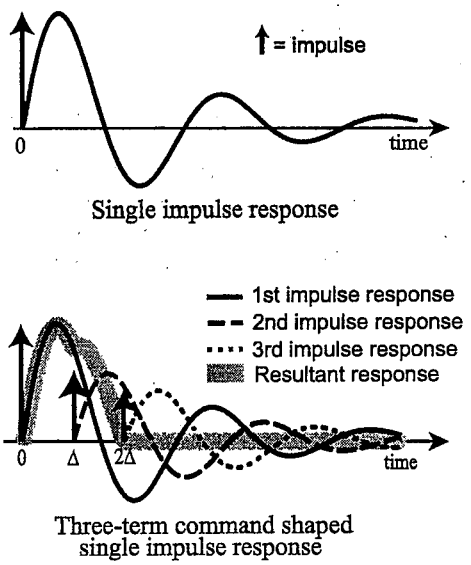

Fig. 6. Elastic response with a three-term command shaper for an impulse input.

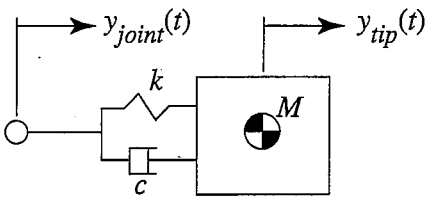

Fig. 7. Simplified flexible gantry robot model used in simulation.

and its predictor can be expressed as

$$\hat{y}_{fd}(n) = y_f(n) = \hat{C}(z,\theta)y(n) = \theta^T(n)\psi(n) \qquad (24)$$

where $\theta^T(n) = [c_0(n)\ c_1(n)\ c_2(n)]$ and $\psi^T(n) = [y(n)\ y(n-\Delta)\ y(n-2\Delta)]^T$ which is measurable. Comparing this system with (10), we get

$$\hat{G}(z,\theta) = \hat{C}(z,\theta), \quad \hat{H}(z,\theta) = 1. \qquad (25)$$

Then the cost function using the quadratic norm of the error $\varepsilon(n)$ is expressed as

$$J(N) \approx \frac{1}{N}\sum_{k=0}^{N-1} |C_d(e^{j\omega}) - \hat{C}(e^{j\omega},\theta)|^2 \left|Y\left(W_N^k\right)\right|^2. \qquad (26)$$

Notice that the cost function does not have the adverse weighting caused by the denominator dynamics of the system. The reason is that in the direct adaptive command shaping

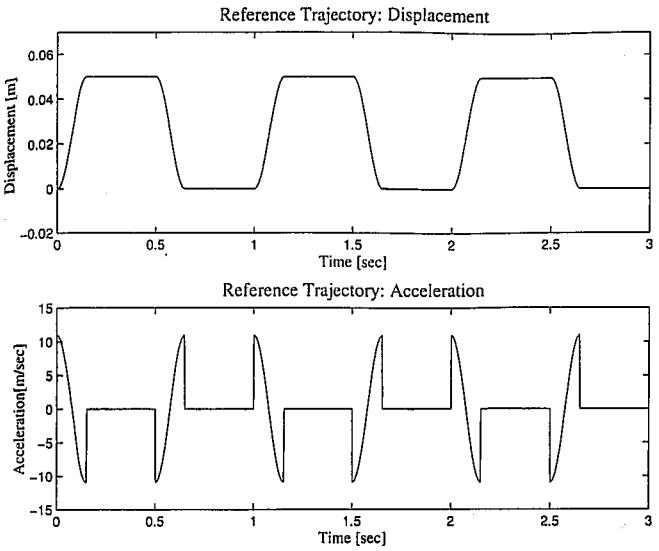

Fig. 8. Reference input trajectory for joint.

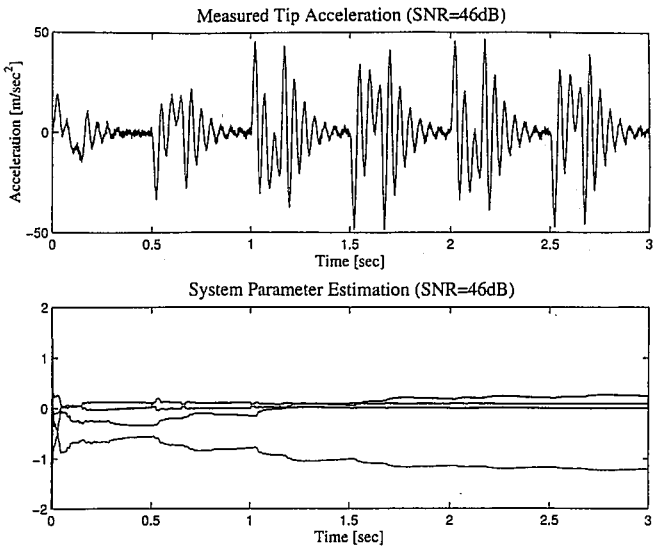

Fig. 10. Indirect adaptation simulation results with noise level II.

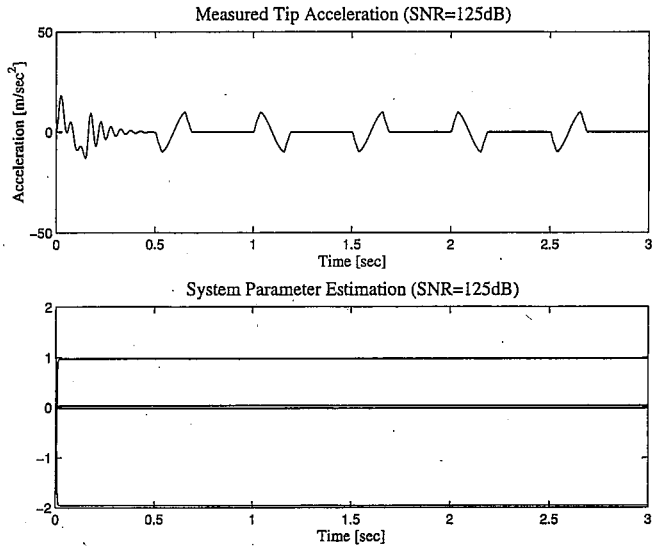

Fig. 9. Indirect adaptation simulation results with noise level I.

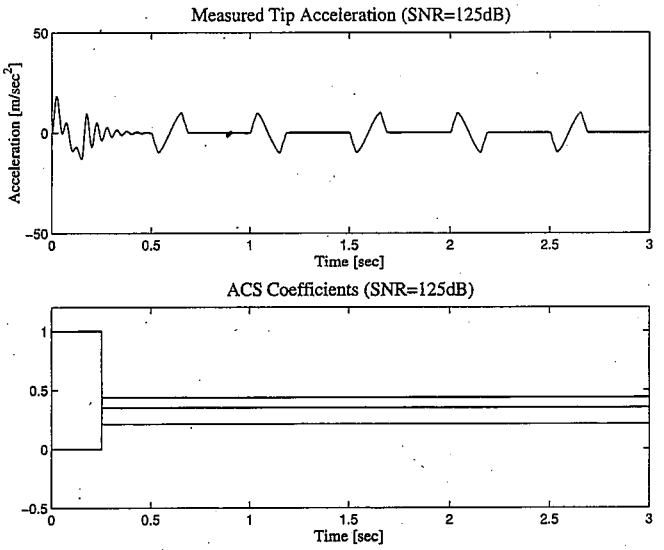

Fig. 11. Direct adaptation simulation results with noise level I.

approach, we estimate the coefficients of the desired FIR filter that does not have denominator dynamics. Therefore, the direct adaptive command shaping is less sensitive to the noise in the system. In addition to that, in the cost function, the plant output spectrum $|Y(W_N^k)|^2$ effectively weights the frequency range where the vibration of the flexible manipulator output $y(n)$ persists. This favorable result is caused by the use of the post-filtering configuration where the flexible manipulator output (tip motion) is used as the input to the adaptive algorithm.

Now, let us consider the desired response $y_{fd}(n)$ which is expressed as

$$y_{fd}(n) = C_d(z)G_{cl}(z)r(n) \tag{27}$$

where $G_{cl}(z)$ is the transfer function of the flexible manipulator system. Obviously, it is not possible to decide $y_{fd}(n)$ without knowing $C_d(z)$ and $G_{cl}(z)$. However, there is a unique characteristic of $C_d(z)$ that allows us to decide $y_{fd}(n)$ in the residual period. This is illustrated using the impulse response of a lightly damped second-order system with/without the command shaping in Fig. 6. When the impulse input filtered by the ideal command shaper $C_d(z)$ is applied to a lightly damped second-order system, there is a nonzero transient response between time 0 and 2Δ (command shaper length) that cannot be decided without knowing the elastic system and the command shaper. However, after 2Δ the resultant vibration in the residual period where the desired acceleration is zero should be zero. Based on this partial information about the desired response, we utilize only the residual period for the adaptation. The residual period can be identified beforehand from the readily available reference input $r(n)$ and prefixed Δ.

Among many types of adaptive algorithms based on the least squares cost function, we have chosen to use the RLS method, for its ease of analysis, effective performance, relatively fast convergence rate and convergence independent of input characteristics. The RLS algorithm produces an asymptotically unbiased estimate of optimal solution to the minimization of (12) [4].

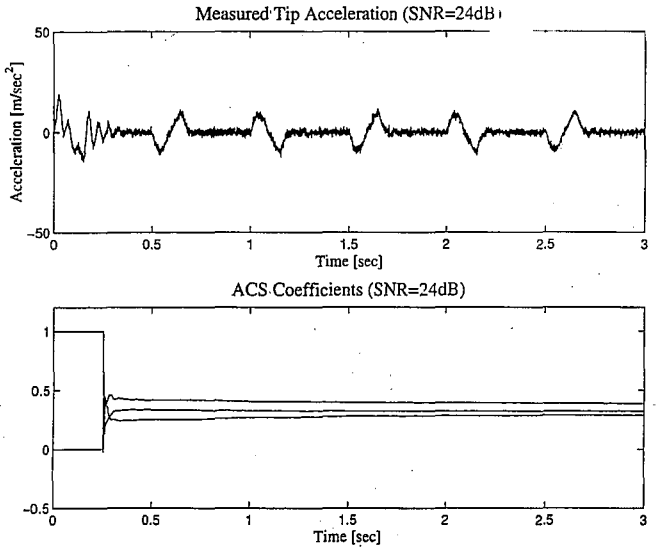

Fig. 12. Direct adaptation simulation results with noise level II.

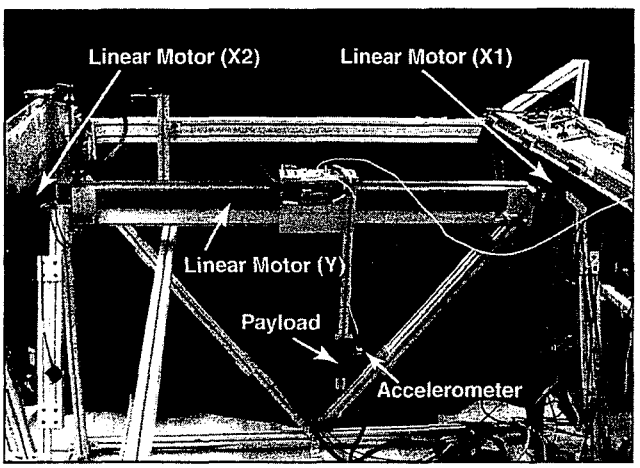

Fig. 13. Test bed: schematic view and picture of actual system.

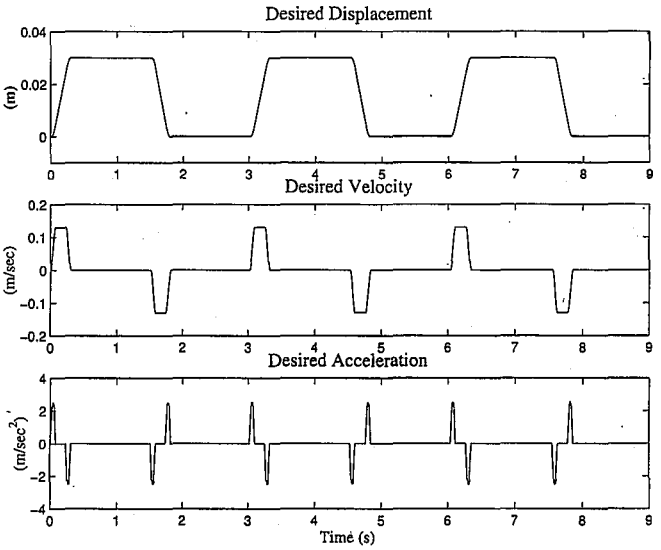

Fig. 14. Reference trajectory used in experiment.

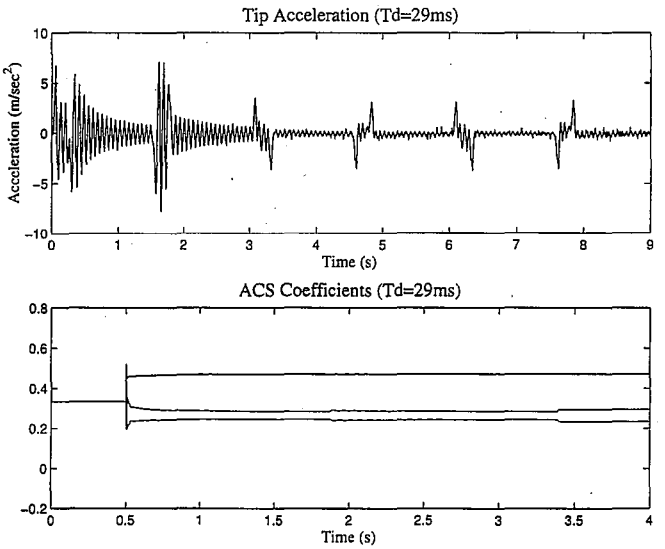

Fig. 15. Measured tip acceleration and change of ACS coefficients from experiment (T_d = 29 ms).

In the direct adaptive command shaping approach, however, the standard RLS algorithm should be modified to satisfy the unit dc gain constraint (28).

$$\mathbf{h}^T\theta(n) = 1, \quad \mathbf{h}^T \equiv [1 \quad 1 \quad 1]. \tag{28}$$

Finally, linearly constrained recursive least squares (LCRLS) to find an updated adaptive command shaper (ACS) coefficient vector $\theta(n)$ at each discrete time n are listed in (29)–(31).

$$\mathbf{k}(n) = \frac{\mathbf{P}(n-1)\psi(n)}{1+\psi^T(n)\mathbf{P}(n-1)\psi(n)} \tag{29}$$

$$\mathbf{P}(n) = [\mathbf{P}(n-1) - \mathbf{k}(n)\psi^T(n)\mathbf{P}(n-1)] \tag{30}$$

$$\theta(n) = \frac{\mathbf{P}(n)\mathbf{h}}{\mathbf{h}^T\mathbf{P}(n)\mathbf{h}} \tag{31}$$

where $\mathbf{P}^{-1}(n) = \sum_{i=1}^{n}\psi(i)\psi^T(i)$ and the initial condition for $\mathbf{P}(n)$ can be decided in the same way as in the standard RLS method [4].

V. Simulation

To verify the analytic result shown in the previous section, simulation has been performed and the results are compared in this section. For the simulation, as shown in Fig. 7, we used a simplified model of the gantry type robot with a flexible link where only one elastic mode with 20 Hz natural frequency is included. In this modeling, we assume that the joint perfectly follows the given desired displacement $y_{\text{joint}}(t)$ to get rid of the controller effects in the following comparisons. The transfer function of the model in s-domain is shown in (32)

$$G_{\text{sim}}(s) \equiv \frac{Y_{\text{tip}}(s)}{Y_{\text{joint}}(s)} = \frac{2\zeta\omega_n s + \omega_n^2}{s^2 + 2\zeta\omega_n s + \omega_n^2} \tag{32}$$

where $y_{\text{joint}}(t)$ and $y_{\text{tip}}(t)$ represent the displacement of the joint and the tip of the link, respectively. A repetitive reference input trajectory shown in Fig. 8 is used in the simulation. To

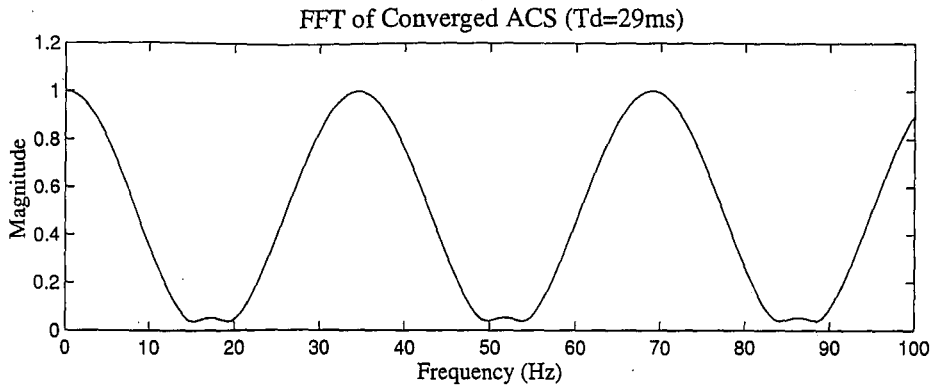

Fig. 16. Frequency response magnitude of converged ACS from experiment ($T_d = 29$ ms).

match with the practical environment where the direct measurement of the accelerations are readily and unobtrusively available, in the simulation, the accelerations $\ddot{y}_{\text{joint}}(t)$, $\ddot{y}_{\text{tip}}(t)$ are used instead of the displacements for the adaptive algorithms. The tip acceleration represents the tip vibration just as well as the displacement does (except for the magnitude difference). To observe the response of the two adaptive approaches to the noise, two different levels of random zero mean measurement noise were used in the simulation (Noise level I: $\sigma^2 = 10^{-5}$ and Noise level II: $\sigma^2 = 1.0$, where σ^2 represents the power of noise). The sampling frequency is set to 1 kHz. In both approaches, the coefficients of adaptive command shapers are updated only at the residual period to avoid the convolution problems related to the varying command shaper coefficients [7].

A. Indirect Adaptive Approach

The ARX model of the plant for the system estimation is chosen as

$$\hat{G}_{\text{sim}}(z,n) \equiv \frac{\hat{B}(z,n)}{\hat{A}(z,n)} = \frac{b_1(n) + b_2(n)z^{-1}}{1 + a_1(n)z^{-1} + a_2(n)z^{-2}} \quad (33)$$

and the predictor can be express as

$$\begin{aligned}\hat{y}(n) &= \hat{B}(z,n)u(n) + [1 - \hat{A}(z,n)]y(n) \\ &= \theta^T(n)\psi(n)\end{aligned} \quad (34)$$

where $\theta^T(n) = [-a_1(n) \;\; -a_2(n) \;\; b_1(n) \;\; b_2(n)]$ and $\psi^T(n) = [\ddot{y}_{\text{tip}}(n-1) \;\; \ddot{y}_{\text{tip}}(n-2) \;\; \ddot{y}_{\text{joint}}(n-1) \;\; \ddot{y}_{\text{joint}}(n-2)]$. As mentioned above, the sampled accelerations are used for the regressor $\psi(n)$ instead of the displacement. The recursive least squares method is used to update $\theta(n)$, which produces an asymptotically unbiased estimate of optimal solution to the minimization of the cost function. From the updated $\theta(n)$, the new estimation of the natural frequency and the damping ratio of the system is extracted. Then, these values are used to calculate the three coefficients of the command shaper with fixed time delay at 20 ms. Initially, the command shaper has a coefficient vector of [1 0 0] which means no command shaping. The simulation results are listed in Figs. 9 and 10. Each of those figures has plots of the measured tip acceleration and $\theta(n)$.

B. Direct Adaptive Approach

The model of a command shaper with fixed time delay of 20 ms is shown below

$$\hat{C}(z,n) = \hat{c}_0(n) + \hat{c}_1(n)z^{-\Delta} + \hat{c}_2(n)z^{-2\Delta} \quad (35)$$

where $\sum_{i=0}^{2} \hat{c}_i = 1$ (unity gain constraint). The predictor model can be expressed as

$$\hat{y}(n) = \theta^T(n)\psi(n) \quad (36)$$

where, $\theta^T(n) = [c_0(n) \;\; c_1(n) \;\; c_2(n)]$ and $\psi^T(n) = [\ddot{y}_{\text{tip}}(n) \;\; \ddot{y}_{\text{tip}}(n-1) \;\; \ddot{y}_{\text{tip}}(n-2)]$. The sampled acceleration of the tip is used for the regressor. Adaptation follows the method described in the previous section. Simulation results using the direct approach are shown in Figs. 11 and 12. Each of those figures has plots of the measured tip acceleration and $\theta(n)$. Agreeing with the analytical result, the simulation results show that the direct approach is less sensitive to the noise.

VI. Experiment

Experiments using the direct adaptive command shaper have been performed. The flexible manipulator system we have used in our experiments is the gantry-type robot shown in Fig. 13. The post adaptive filtering configuration has been implemented on this test bed. The manipulator system has three prismatic joints. The X1 and X2 joints constrain the motion of the horizontal beam to be along the tracks of two linear motors in the x-direction. The Y joint constrains the motion of the base of the vertical flexible probe to be along the linear motor that is fixed on the horizontal beam, in the y-direction. A 2-kg payload is attached at the tip of the vertical flexible probe. The displacements of the joints are measured with encoders. Accelerometers attached at the tip of the vertical flexible link to measure the tip vibration in the x and y direction. The measured tip acceleration is used to adapt the command shaper in the experiments.

In this paper, we only show the experimental results related to the x-directional motion. The tip vibration in the x-direction is to be suppressed by the adaptive command shaper. The manipulator has a single dominant elastic mode in the x-direction, with a natural frequency of 15 Hz. The two sides of the horizontal beam (X1 and X2) are driven by two separate independent PD

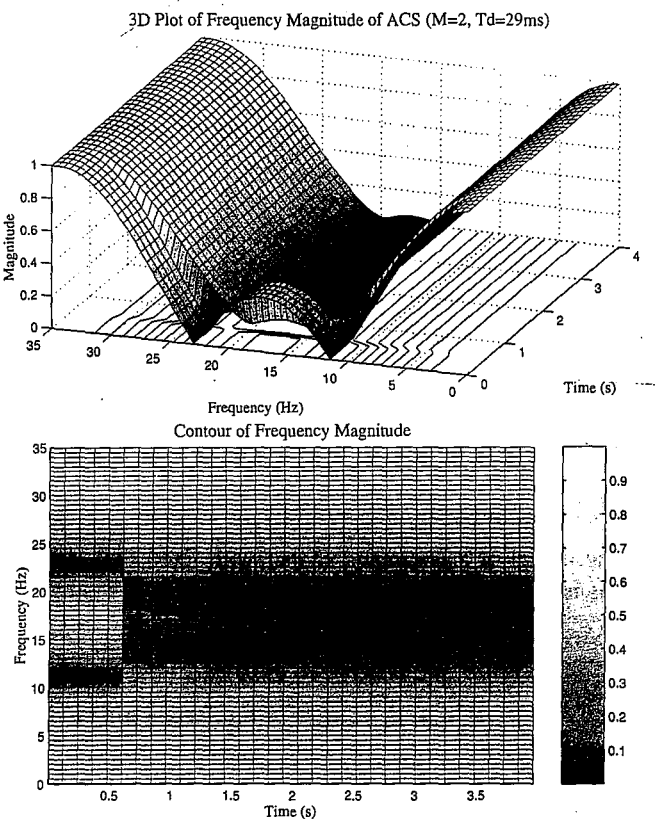

Fig. 17. Three-dimensional plot of frequency response magnitude of ACS from experiment and its contour ($T_d = 29$ ms).

controllers using a 1 kHz sample rate. While running the experiment for the x-directional motion, the base of the vertical flexible probe is kept at the middle of the horizontal beam. The same periodic trapezoidal velocity trajectory shown in Fig. 14 is used as the reference input for the X1 and X2 joints. The same command shaper is also used for the two joints and the same adaptive command shaper is used for both joints. Assuming that we do not have knowledge about the flexible system parameters, we have tested several time-delay values for the ACS. All of them showed very similar results, and only a single set of experimental results where the time-delay is set to be 29 ms are listed in this paper. In all these experiments, the ACS algorithm is turned on at the beginning of the first residual period. The initial value of $\mathbf{P}(0)$ has been chosen to be a diagonal matrix, $\text{diag}(p_0, p_0, p_0)$, where $p_0 = 10^7$ and the initial value of $\theta(0)$ is $[1/3\ 1/3\ 1/3]^T$. The transmission of the adapted command shaper coefficients of $\hat{C}(z,n)$ to $C(z,n)$ which actually filters the command has been initiated after one cycle of the trajectory which is 3 s. After 3 s, every new ACS coefficient calculated is transmitted to $C(z,n)$ at every sample time during the residual period. Before the transmission begins, $C(z,n)$ is kept at unity, which means no command shaping.

Fig. 15 shows the measured tip acceleration (top plot) and the adaptation of $\theta(n)$ (bottom plot). We observe the significant reduction of the residual vibration down to the environmental noise level after the transmission of the ACS coefficients are initiated. Fig. 16 is the magnitude plot of the frequency transform of the converged ACS at the end of adaptation. Fig. 17 shows the three-dimensional plot of the frequency transform of $\theta(n)$ and its contour map. The contour map shows the changes of the magnitude of the frequency transform of the ACS during the adaptation. Figs. 16 and 17 show the local minimum around the natural frequency of the elastic mode at 15 Hz.

VII. Conclusion

In this paper, we have analyze the noise effect on the performance of two time-domain adaptive command shaping approaches (indirect, direct). The analysis shows that the direct approach is less sensitive to the noise. This result is supported by the proper simulation using four different levels of noise. Finally, experimental results verify the effectiveness of the direct command shaping approach.

Acknowledgment

The authors thank to the flexible manipulator control workgroup in the Georgia Institute of Technology for their help and advice pertaining to this work.

References

[1] W. J. Book, D. P. Magee, and S. Rhim, "Time-delay command shaping filters: Robust and/or adaptive?," *J. Robot. Soc. Japan*, vol. 17, no. 6, pp. 761–769, 1999.

[2] M. Bodson, "An adaptive algorithm for the tuning of two input shaping methods," *Automatica*, vol. 34, no. 6, pp. 771–776, 1998.

[3] F. Khorrami, S. Jain, and A. Tzes, "Experimental results on adaptive nonlinear control and input preshaping for multilink flexible manipulators," *Automatica*, vol. 31, no. 1, pp. 83–97, 1995.

[4] S. Haykin, *Adaptive Filter Theory*. Englewood Cliffs, NJ: Prentice-Hall, 1996.

[5] L. Ljung, *System Identification: Theory for the User*. Engelwood Cliffs, NJ: Prentice-Hall, 1987.

[6] D. P. Magee and W. J. Book, "Optimal filtering to minimize elastic behavior in serial link manipulators," in *Proc. Amer. Contr. Conf.*, Philadelphia, PA, June 24–26, 1998, pp. 2637–2642.

[7] ——, "The application of input shaping to a system with varying parameters," in *Proc. Japan/USA Symp. Flexible Automat.*, vol. 1, San Francisco, CA, July 13–15, 1992, pp. 519–526.

[8] J. Park and P.-H. Chang, "Learning input shaping technique for non-LTI systems," in *Proc. Amer. Contr. Conf.*, Philadelphia, PA, June 1998, pp. 2652–2656.

[9] S. Rhim and W. J. Book, "Adaptive command shaping using adaptive filter approach in time domain," in *Proc. Amer. Contr. Conf.*, vol. 1, San Diego, CA, June 2–4, 1999, pp. 81–85.

[10] D. M. Rovner and R. H. Cannon Jr., "Experiments toward on-line identification and control of a very flexible one-link manipulator," *Int. J. Robot. Res.*, vol. 6, no. 4, pp. 3–19, 1987.

[11] N. Singer, W. Singhose, and W. Seering, "Comparison of filtering methods for reducing residual vibrations," Eur. J. Contr., to be published.

[12] W. Singhose, N. Singer, and W. Seering, "Residual vibration reduction using vector diagrams to generate shaped inputs," *J. Mech. Design*, pp. 654–659, June 1994.

[13] N. C. Singer and W. P. Seering, "Preshaping command inputs to reduce system vibration," *J. Dyn. Syst., Measurement, Contr.*, vol. 112, no. 1, pp. 76–82, 1990.

[14] A. Tzes and S. Yurkovich, "An adaptive input shaping control scheme for vibration suppression in slewing flexible structures," *IEEE Trans. Contr. Syst. Technol.*, vol. 1, pp. 114–121, June 1993.